THEORETICA CHIMICA ACTA
Theoret. Chim. Acta (Berl.) 58, 257–283 (1981)

Electronic Band Structures and Electronic Properties of Some Substituted Linear Polyenes

E. A. Cetina, V* and Peter G. Perkins

Department of Pure and Applied Chemistry, University of Strathclyde, Glasgow G1 1XL, Scotland

A series of linear polyenes having the side groups, Cl, Me, CN, Ph, and —PhOMe, has been studied by a self-consistent LCAO tight-binding method. It is found that, with normal bond lengths, several of these materials are predicted to be electronic conductors in the solid state. This property is lost, however, when the lattice vector is increased. Of particular interest are the phenyl- and phenoxy-substituted compounds where the rings form conducting paths by transannular overlap. Energy transfer and the effects of disorder and segmental rotation of the backbone are also considered.

Key Words: Linear polyenes – Band structure – Transport properties.

1. Introduction and Method

Polymers containing unsaturated —CR=CR— units in the main chain have proved to possess interesting physical properties which may lead to possible practical utilisation. A particularly exciting discovery is that doping of polyenes with foreign atoms can lead to remarkable changes in their electrical conductances [1–4]. A full experimental study of these polymers is beset by difficulties and, hence, a theoretical approach could be fruitful to point the way that these properties can be understood and systematically exploited. There have been some investigations in this area which have revealed interesting phenomena of general importance for macromolecular chemistry, e.g. efficient energy-transfer processes and the possibility of organic superconductors and materials which will collect light over a wide energy range [5, 6].

* Instituto de Investigaciones de Materiales, Universidad Nacional Autónoma de México, Apartado Postal 70-360, Ciudad Universitaria, México 20, D.F., México.

0040-5744/81/0058/0257/$05.40

Since the above-type properties of these conjugated systems stem, in general, from the overlap of π orbitals oriented in some way along the chain, and since this overlap is a maximum in a co-planar arrangement of the unit cells of the polyene chain, it is of interest to ascertain the geometrical dependence of the properties and how they are affected when the co-planarity is perturbed.

Band theory has already been of considerable help in the study of these conjugated polyene chains [7]. In some previous investigations [7], the Hückel theory [9] has been employed to compute properties of conjugated polymer crystals. However, in Hückel theory, electron-electron interaction is neglected as the Hamiltonian remains undefined and so questions must arise as to the validity of the results obtained with such an approach. Self-consistent methods have been found to give a good account of the electronic properties of carbon-containing molecules [10] and early attempts [7, 8] to calculate the band structures of polycarbon chains were encouraging. It is, therefore, clearly desirable to apply these methods to the more general study of polyene chains.

The best theoretical approach is clearly to carry out geometry optimisation on all bond angles and lengths employing an *ab initio* molecular-orbital procedure and, indeed, some progress has been made in this direction [7, 11]. However, such an approach is impracticable when the polymer possesses the type of substituted side group which, in general, lends stability to the systems. We believe, therefore, that, with all the above in mind, an approach at the CNDO level of sophistication is likely to yield results which will afford reasonably reliable qualitative and even perhaps semi-quantitative information about the likely properties of these systems.

1.1. Method of Calculation

The method of calculation employed is based on a tight-binding LCAO approach and is a modified CNDO method which has been successfully used to study the properties of some symmetrical solids [12]. Some significant computational changes have been made to improve the performance of this method and, hence, a brief resumé of the original is presented. In general terms, the matrix elements $F_{\lambda\lambda}$ and $F_{\lambda\sigma}$ of the Hartree–Fock Hamiltonian are given by,

$$F_{\lambda\lambda} = -I_{\lambda\lambda} + (1 - \tfrac{1}{2}P_{\lambda\lambda})\gamma_{AA} + M'_{\lambda\lambda} \tag{1}$$

$$F_{\lambda\sigma} = -AS_{\lambda\sigma}(I_{\lambda\lambda}I_{\sigma\sigma})^{1/2} - \tfrac{1}{2}P_{\lambda\sigma}\gamma_{AB} \tag{2}$$

where $I_{\lambda\lambda}$ is the valence-state ionisation potential for the atomic orbital ϕ_λ, $P_{\lambda\sigma}$ represent the iterating density matrix elements,

$$P_{\lambda\sigma} = 2 \sum_{i(\text{occ})} c^*_{\lambda i}\, c_{\sigma i} \tag{3}$$

the diagonal elements given by Eq. (3) are the so-called bond orders between the pairs of orbitals involved, $c_{\lambda i}$ are the coefficients for the ith molecular orbital, γ_{AA} is the electrostatic repulsion integral between two electrons in any one of the valence orbitals of atom A, γ_{AB} is the average electrostatic repulsion integral

between any electron in the valence orbitals of atom A and any electron in the valence orbitals of atom B, A is the Mulliken–Wolfsberg–Helmholtz (MWH) constant, $S_{\lambda\sigma}$ is the overlap integral between the atomic orbitals ϕ_λ and ϕ_σ,

$$S_{\lambda\sigma} = \langle \phi_\lambda | \phi_\sigma \rangle \tag{4}$$

and

$$M'_{\lambda\lambda} = \sum_\sigma (P_{\sigma\sigma} - P^g_{\sigma\sigma}) \gamma_{AB} \tag{5}$$

given in terms of the atomic population in ϕ_σ in the free atom, $P^g_{\sigma\sigma}$ represents the constant potential-energy term which arises from the charge separation in the system.

Now, under the CNDO approximations Eqs. (1), (2), (3) and (4) are given, respectively, by,

$$F_{\lambda\lambda}(k) = -I_{\lambda\lambda} + (1 - \tfrac{1}{2}P^{00}_{\lambda\lambda})\gamma^{00}_{AA} + \sum_\sigma (P^{00}_{\sigma\sigma} - P^g_{\sigma\sigma}) \times \sum_{n=-N/2}^{+N/2} \gamma^{0n}_{\lambda\sigma} - \sum_{n=-N/2}^{N/2} \cos(\boldsymbol{k} \cdot \boldsymbol{R}_n)(AI_{\lambda\lambda}S^{0n}_{\lambda\lambda} + \tfrac{1}{2}P^{0n}_{\lambda\lambda}\gamma^{0n}_{\lambda\lambda}) \tag{6}$$

$$F_{\lambda\sigma}(\boldsymbol{k}) = -\sum_{n=-N/2}^{N/2} \exp i(\boldsymbol{k} \cdot \boldsymbol{R}_n)(AS^{0n}_{\lambda\sigma}(I_{\lambda\lambda}I_{\sigma\sigma})^{1/2} + \tfrac{1}{2}P^{0n}_{\lambda\sigma}P^{0n}_{\lambda\sigma}) \tag{7}$$

$$P^{0n}_{\lambda\sigma} = X_m \sum_{\boldsymbol{k}} \sum_{i(\mathrm{occ})} c^*_{\lambda i}(\boldsymbol{k}) c_{\sigma i}(\boldsymbol{k}) \exp i(\boldsymbol{k} \cdot \boldsymbol{R}_n) \tag{8}$$

and,

$$S_{\lambda\sigma}(\boldsymbol{k}) = \sum_{n=-N/2}^{N/2} \exp i(\boldsymbol{k} \cdot \boldsymbol{R}_n) S^{0n}_{\lambda\sigma} S^{0n}_{\lambda\sigma}. \tag{9}$$

These result from writing the Bloch sum,

$$\psi_\lambda(\boldsymbol{k}) = \frac{1}{\sqrt{N}} \sum_{\boldsymbol{R}_n=0}^{N} \exp i(\boldsymbol{k} \cdot \boldsymbol{R}_n) \phi_\lambda(\boldsymbol{r} - \boldsymbol{R}_n) \tag{10}$$

for the solution of Schrödinger's equation for the system. Here, $\lambda = 1, 2, \ldots, m$ is the number of atomic orbitals per unit cell, $\phi_\lambda(\boldsymbol{r} - \boldsymbol{R}_n)$ is a Slater-type atomic orbital situated at a vector distance $\boldsymbol{R}_n$ from the atomic orbital $\phi_\lambda(\boldsymbol{r} - \boldsymbol{R}_0)$. $\boldsymbol{R}_0$ locates the unit cell taken as the central unit cell, N represents the total number of unit cells in the system, $\boldsymbol{R}_n$ is the linear translation vector. The label $\boldsymbol{k}$ specifies the irreducible representation of the translational group to which the Bloch functions belong. The other superscripts 0 and n refer to the position of the cell, thus,

$$S^{0n}_{\lambda\sigma} = \langle \phi_\lambda(\boldsymbol{r} - \boldsymbol{R}_0) | \phi_\sigma(\boldsymbol{r} - \boldsymbol{R}_n) \rangle. \tag{11}$$

In expression (8) the sum over $\boldsymbol{k}$ extends over the central Brillouin zone, the sum over i extends over the occupied band and X_m is a normalisation constant. The secular equations are solved by evaluating the secular determinant,

$$|F_{\lambda\sigma}(\boldsymbol{k}) - \varepsilon_j(\boldsymbol{k})| = 0. \tag{12}$$

The modifications to the above CNDO-based method, which have been incorporated in our calculations, are the following:

(a) It is well known that Eqs. (6) and (7) represent the correct effect on $M_{\lambda\lambda}$ (5) on the molecular-orbital energy level for an orthogonal basis set. In order to be able to use a nonorthogonal basis set which we consider essential for the solid-state problem, since Bloch functions incorporate overlap terms, the following expressions for the off-diagonal matrix elements need to be considered,

$$F_{\lambda\sigma} = -AS_{\lambda\sigma}(I_{\lambda\lambda}I_{\sigma\sigma})^{1/2} - \tfrac{1}{2}P_{\lambda\sigma}\gamma_{AB} + \tfrac{1}{2}S_{\lambda\sigma}(M'_{\lambda\lambda} + M'_{\sigma\sigma}). \tag{13}$$

We believe that this modification gives more valid eigenvalues, since the off-diagonal matrix elements of the overlap matrix are thus taken into account when solving the appropriate secular determinant.

(b) The matrix elements concerning the two-electron part of the Hartree–Fock Hamiltonian were evaluated using γ integrals,

$$\gamma_{\lambda\sigma} = \left\langle \phi_\lambda^2(1) \left| \frac{1}{r_{12}} \right| \phi_\sigma^2(2) \right\rangle \tag{14}$$

where r_{12}^{-1} represents the distance between the centres of the atomic orbitals ϕ_λ and ϕ_σ. For large molecules and solids, the number of γ integrals to be evaluated is very large (the extended Hückel theory simply neglects them). Using an heuristic approach, however, the γ integrals can be included and this, we believe, makes the entire calculation more reliable. The approach consists of representing each atomic orbital by a sphere of suitable radius within which the electron density is uniform and outside which it is negligible. The whole procedure has been detailed elsewhere [13].

(c) An overlap matrix is employed which is calibrated through band structures obtained from *ab initio* methods for polyethylene [16] so, in place of Eq. 4, we use,

$$S'_{\lambda\sigma} = S_{\lambda\sigma}[\delta_{\lambda\sigma} + \alpha(1 - \delta_{\lambda\sigma})] \tag{15}$$

where the "calibration parameter", α [12], lies between unity, its value in *ab initio* methods, and zero, its value in CNDO methods.

The inclusion of (a)–(c) modifies the previous expressions to give,

$$F_{\lambda\lambda}(\boldsymbol{k}) = -I_{\lambda\lambda} + (1 - \tfrac{1}{2}P_{\lambda\lambda}^{00})\gamma_{\lambda\lambda}^{00} + M'_{\lambda\lambda} - \sum_{n=-N/2}^{N/2} \cos(\boldsymbol{k}\cdot\boldsymbol{R}_n)[AI_{\lambda\lambda}S_{\lambda\lambda}^{0n} + \tfrac{1}{2}P_{\lambda\lambda}^{00}\gamma_{\lambda\lambda}^{0n} - S_{\lambda\lambda}^{0n}M'_{\lambda\lambda}] \tag{16}$$

$$F_{\lambda\sigma}(\boldsymbol{k}) = \sum_{n=-N/2}^{N/2} \exp i(\boldsymbol{k}\cdot\boldsymbol{R}_n)[AS_{\lambda\sigma}^{0n}(I_{\lambda\lambda}I_{\sigma\sigma})^{1/2} + \tfrac{1}{2}P_{\lambda\sigma}^{0n}\gamma_{\lambda\sigma}^{0n}] + \tfrac{1}{2}\sum_{n=-N/2}^{N/2} S_{\lambda\sigma}^{\prime 0n}(M'_{\lambda\lambda} + M'_{\sigma\sigma}) \exp i(\boldsymbol{k}\cdot\boldsymbol{R}_n) \tag{17}$$

where $M'_{\lambda\lambda}$, which generally is given as in (5), is now written as,

$$M'_{\lambda\lambda} = \sum_{\sigma} (P^{0n}_{\sigma\sigma} - P^{g}_{\sigma\sigma}) \sum_{n=-N/2}^{N/2} \gamma^{0n}_{\lambda\sigma} \tag{18}$$

$$S'_{\lambda\lambda}(\boldsymbol{k}) = 1 + \sum_{n=-N/2}^{N/2} \alpha \cos(\boldsymbol{k} \cdot \boldsymbol{R}_n) S^{0n}_{\lambda\lambda} \tag{19}$$

and

$$S'_{\lambda\sigma}(\boldsymbol{k}) = \sum_{n=-N/2}^{N/2} \alpha \exp i(\boldsymbol{k} \cdot \boldsymbol{R}_n) S^{0n}_{\lambda\sigma}. \tag{20}$$

The secular determinant to be solved is,

$$|F_{\lambda\sigma}(\boldsymbol{k}) - \varepsilon_j(\boldsymbol{k}) S'_{\lambda\sigma}(\boldsymbol{k})| = 0. \tag{21}$$

In the present work, we have thus carried out SCF calculations of the band structure for the systems shown in Fig. 1. As can be seen from the figure, we have considered calculations with a number of different side groups which are of

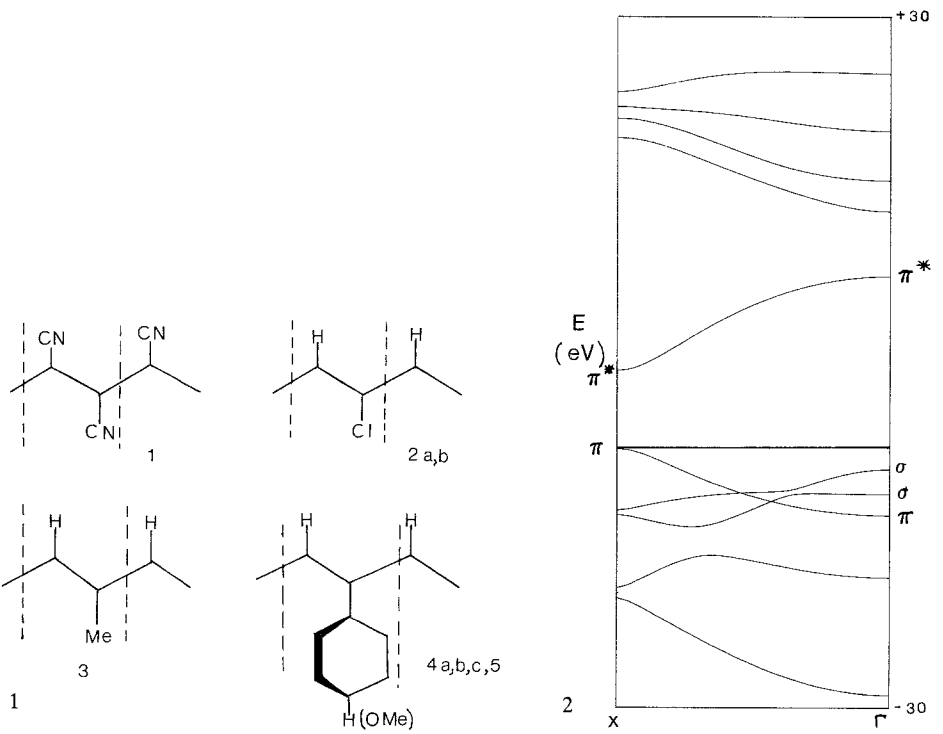

Fig. 1. Models studied. In Models 2b, 4b, and 4c the translation vector was increased to 3 Å. In model 3b the translation vector was 2.65 Å. In models 4a, 4b, and 5 all phenyl rings lie at 90° to the main chain. In model 4c the rings lie at 45° with respect to the main chain

Fig. 2. Band Structure for Polyacetylene

chemical interest. The particular set of substituents was chosen so that the general effects of alkyl groups, atomic, and pseudoatomic substituents, phenyl, and substituted phenyl groups could be uncovered. From these results we would expect to draw some general principles. Where it was geometrically feasible, we have taken the side groups to be co-planar with the main backbone. We have also varied the C—C chain distances from the known literature [14] values in order to reveal how the different induced π overlap alters the properties of the polyenes. Other structural parameters were maintained at standard values [14]. In all cases the double and single bonds were given alternating lengths (*vide infra*). In the case of system 1, the properties were found to be insensitive to a reasonable variation of the C—C chain distances, hence only results for the standard geometry are reported. For system 2 we also report the properties for those values of the C—C distance for which the system changes drastically its qualitative behaviour. For systems 4 and 5, complete co-planarity of all atoms is not possible without severe clashing of carbon atoms and so we have varied the degree of deviation of the rings from co-planarity as well as the C—C chain vector.

2. Results and Discussion

The unit cells for each system are defined by the dashed vertical lines in Fig. 1. In each case, the translation vector obtained from the interatomic distances given in the literature has length of 2.426 Å, although in cases 2*b*, 4*b*, and 4*c* other geometrical variations were made (see Fig. 1). Opinion [7] generally favours the "alternating bond" nature of these polyenes caused by a Peierls distortion [7] of the equal bond structure: this relieves the symmetry-dictated degeneracy at the outer edge of the Brillouin Zone. Moreover, recent careful *ab initio* calculations [7] on the chain confirm the stability of the alternating-bond structure. The latter calculations were published after the main part of our work was finished and, from the data in that Paper, one can deduce a translation distance of 2.479 Å. In order to check that this slightly longer translation vector (0.053 Å) makes no essential difference to our conclusions, we recalculated the band structures for the chloro- and phenyl-substituted chains (*vide infra*). The results of this comparison are to be found under the appropriate heading for each system. Unit cells enclosed by a 15 Å radius of the central unit all were included in the interaction. The orbital exponents for the Slater-type orbitals used were calculated both from Burn's rules [15] and from relevant *ab initio* methods [16]. The valence-state ionisation potentials required were obtained from spectral data [17]. The MWH constant, which scales the off-diagonal matrix elements, was set at 1.4 [12]. Table 1 lists all the input data used.

The band structures for all systems are shown in Figs. 2–10. The corresponding Fermi level (*vide infra*) and the nature of the orbitals at Γ and X bordering the Fermi level are shown for each of the important bands. Using the band-curvature characteristics the effective masses $\boldsymbol{m}^*$ for electrons and holes in the π bands have been calculated; for systems 3 and 4, both the bands stemming from the π backbone orbitals and the transannular benzene bands have been included in the analysis.

Table 1. Input data

	Orbital exponent	V.S.I.P (eV)	$\gamma_{\mu\mu}$
Carbon			
2*s*	1.608	19.44	15.601
2*p*	1.568	10.67	
Nitrogen			
2*s*	1.875	25.58	18.873
2*p*	1.650	13.19	
Chlorine			
3*s*	2.183	25.29	
3*p*	1.733	13.99	15.334
3*d*	1.000	2.20	
Oxygen			
2*s*	2.200	32.38	22.144
2*p*	1.975	15.85	

The density-of-states function $g(E)$, defined as the number of available states per unit volume per unit energy interval for band j, and given by,

$$g(E)=\frac{2}{8\pi^3}\int \delta[\varepsilon_j(\boldsymbol{k})-E]\,d\boldsymbol{k}$$

has been calculated for each system. This leads to values for the Fermi energy. The calculated effective masses for all the polymers are listed in Table 2.

The extended-band electronic conductivity σ was obtained using [18]

$$\sigma=\frac{2\pi^2 e^2 \hbar^3 \boldsymbol{a}}{\boldsymbol{m}^\star} G(E_F)^2 \tag{22}$$

where $G(E_F)$ is the density of states at the Fermi energy level for the band in question, $\boldsymbol{a}$ is the lattice vector. The value of the electron mobility is then [18]

$$\mu=\frac{\sigma}{G(E_F)\boldsymbol{k}T}. \tag{23}$$

For convenience, T was assumed to be 300 K. The mobilities appear in Table 2.

It is convenient to consider the results system by system and then to draw general conclusions and inferences.

2.1. Topology of Band Structures

2.1.1. Polyacetylene

Figure 2 shows the band structure of the parent material. The alternating bond length assures a band gap which, by symmetry, cannot exist in the system where the bond lengths are equal, since the bands must be degenerate at the point X. The band structure obtained using the translation vector calculated from Karpfen's work [7] was superimposable on that obtained with the vector equal to 2.426 Å.

Table 2. Calculated electronic properties of the polymers

	Density	$N(E_F)\times10^{34}$	Effective Masses electrons	holes	Conductivity, $\sigma(\Omega^{-1}\,cm^{-1})$ electrons	holes	Mobility, $\mu(cm^2\,V^{-1}\,sec^{-1})$ electrons	holes
Polyacetylene (insulator)	1.16	0.60[a]	0.22	0.32	1.4×10^5	0.6×10^5	0.6×10^3	0.3×10^2
Polycyano acetylene (insulator)	—	—	0.21	0.39	—	—	—	—
Polymethyl acetylene (insulator)	—	—	0.26	0.83	—	—	—	—
Polychloro acetylene (insulator)	—	—	0.98	1.03	—	—	—	—
Polychloro acetylene (conductor)	1.4[b]	3.14	0.13	0.14	1.0×10^7	0.84×10^6	0.2×10^4	0.1×10^4
Polyphenyl acetylene (insulator)	—	—	0.73	1.19	—	—	—	—
Polyphenyl acetylene (conductor)	1.12[c]	1.16	0.17 0.29[d]	0.17 —	8.2×10^5	8.0×10^5	1.1×10^4	1.0×10^4
Poly-*p*-methoxy acetylene (conductor)	1.12[c]	6.7	0.18	0.18	2.3×10^7	2.3×10^7	0.5×10^5	0.5×10^5

[a] The density of states at the Fermi level is assumed equal for electrons and holes. The values assume injected electrons giving 1 state per 0.1 eV at E_F.
[b] Assumed to be the same as for polyvinylchloride, Ref. [24].
[c] Assumed to be the same as for polystyrene, Ref. [24].
[d] This value refers to the "backbone" π band.

Table 3. Calculated conductivities and mobilities for polychloro and polyphenyl acetylene

	$\sigma(\Omega^{-1}\,\mathrm{cm}^{-1})$				$\mu(\mathrm{cm}^2\,\mathrm{V}^{-1}\,\mathrm{sec}^{-1})$			
	From Fermi surface		From optical scattering		From Fermi surface		From optical scattering	
	Electrons	Holes	Electrons	Holes	Electrons	Holes	Electrons	Holes
PCA	5.3×10^3	as for electrons	3.0×10^4	5.2×10^4	1.4×10^2	—	7.9×10^2	1.3×10^3
PPA	5.0×10^2		—	—	6.5	—	—	—

We discuss the former. The general topological features of this band structure (Table 3) are similar to those previously calculated [7], although it is noticeable that the band widths are in very much better accord with *ab initio* calculations [7] than those of previous CNDO-based methods [8]. Hence, we may reasonably suppose that our present method is acceptably good. The most noticeable feature is the pair of broad π bands which are separable from the σ system and give rise to the suggested transport properties in this and related systems. For brevity we will not discuss this structure further, using it merely as an index for the bands in more complicated structures. The effective masses, $\boldsymbol{m}^\star$, for electrons and holes were, however, calculated and are given in Table 2. These values refer, of course, to injected carriers.

2.1.2. Chlorosubstituted Polyacetylene

In this case the unit cell is as shown in Fig. 1. Three calculations were performed, two in which the lattice vectors were 2.479 Å [7] and 2.426 Å, respectively, and one where the vector was increased, for the reasons quoted earlier, to 3.0 Å. The results of the first two calculations were virtually indistinguishable and we describe those stemming from the 2.479 Å translation vector. The band structures show a remarkable difference between the calculated properties of these two systems (Figs. 3 and 4). A glance suffices to show that the material is an insulator with an appreciable band gap when the repeat distance is 3 Å but when this distance is decreased, the picture alters dramatically and the material becomes a conductor. Analysis of the band topology for the two systems reveals the root cause of the difference. In the insulator the bands bordering the gap are the readily identifiable π bands of the main chain (correlatable with Fig. 2) although, of course, somewhat narrowed and changed by the long repeat distance and the participation of the Cl $3p_\pi$ orbitals. In the conductor, the π conduction band is dramatically widened and its eigenvalue at $\boldsymbol{k} = \pi/\boldsymbol{a}$ dramatically lowered. This, of itself, would not cause the material to be a conductor but the change in the π band is accompanied by a remarkable upthrust in the energy of the Cl p_σ band at the Γ point. This latter band is formed from the Cl p_σ orbitals which point in a direction parallel with the main chain and so mutually interact in direct 1:1 σ fashion. It is significant that the inter-chlorine distance in this system is very little greater than twice the covalent radius of chlorine. Moreover, this particular set of chlorine p

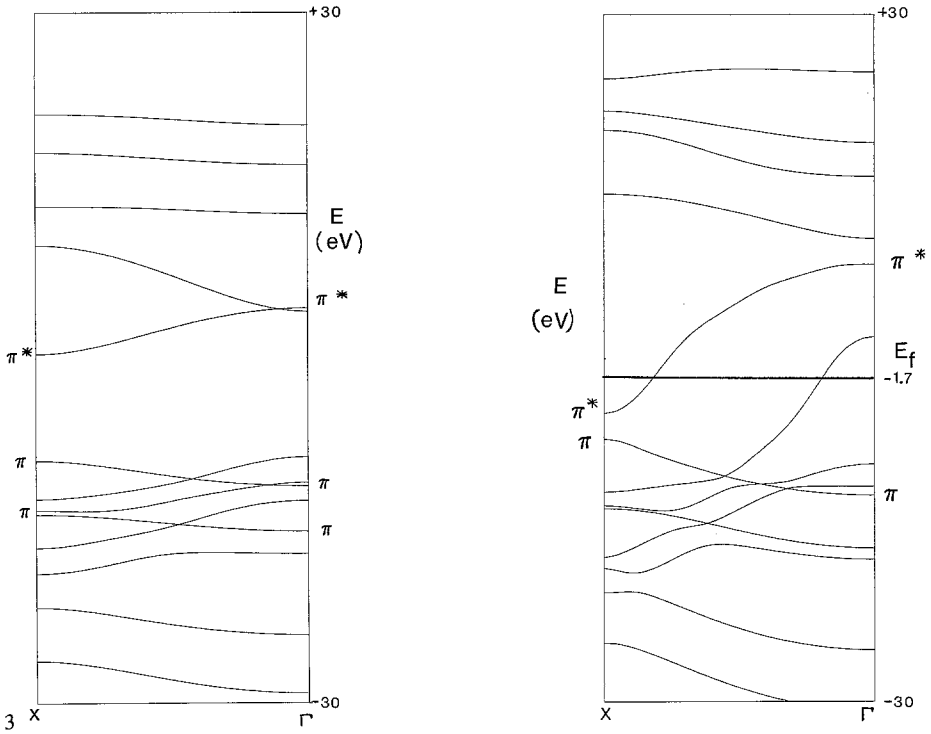

Fig. 3. Band Structure for Polychloroacetylene, $t = 3.0$ Å
Fig. 4. Band Structure for Polychloroacetylene, $t = 2.479$ Å

orbitals are almost independent of the bonding of the atom to the backbone chain. Strong band overlap between formal σ valence and π conduction bands occurs and confers the open-band properties.

A p_σ band is also extant in the saturated material polyvinylchloride and is considered to confer the electron donor properties which that material exhibits [8]. However, in the latter, the average interchlorine distance is lengthened by free rotation and, moreover, there is no strong π conduction band emanating from the main chain (the conduction bands are quite flat). Furthermore, the chlorine atoms are not coplanar with the main chain and the carbon atoms to which they are bonded are also "taken up" with attached hydrogens. Hence, it is not surprising that no electronic conductance is observed for this material.

The density-of-states calculation for polychloroacetylene allows the assignment of a Fermi level which lies high in the valence σ band. The curvature of the two conduction bands (for holes and electrons) allows computation of the relevant effective masses and the extended band mobilities for the carriers (Table 2). The model chosen, that of an isotactic polymer, is, no doubt, an idealised one and perturbations to the geometry are discussed later (*vide infra*). However, it is important to find out, in the limit of an idealised model, what electronic behaviour is possible. Full substitution of hydrogen does not affect the model significantly

because, if the chain were substituted on both sides, we would get essentially a doubling-up of the bands and a minor splitting of these due to the cross-backbone Cl—Cl interaction. We observe this effect in the next case.

2.1.3. Polycyanoacetylene

In this case, every hydrogen atom of the chain was substituted by a cyano group and the translation vector is 2.426 Å. It is notable first of all (Fig. 5) that the material is an insulator, although the presence of two cyano groups increases the symmetry of the system over that of the chloro-compound and several of the bands are near-degenerate at the X point. These are chiefly the bands mainly concerned with the cyano groups. Again, the two π bands stemming from the main chain are clearly extant though, of course, modified by interaction with the cyano π system. It is interesting that, at Γ, there is a pair of high-lying σ valence bands associated with the cyano group. The cyano bands also stabilise the system by displacing the π valence bands downwards.

The reason for the difference in behaviour of this system as against the corresponding chloro material stems from the nature of the cyano group. The prerequisites for the conducting behaviour stem from the orbital and mutual-overlap characteristics of the appended atom. Thus, whereas the Cl atom has large

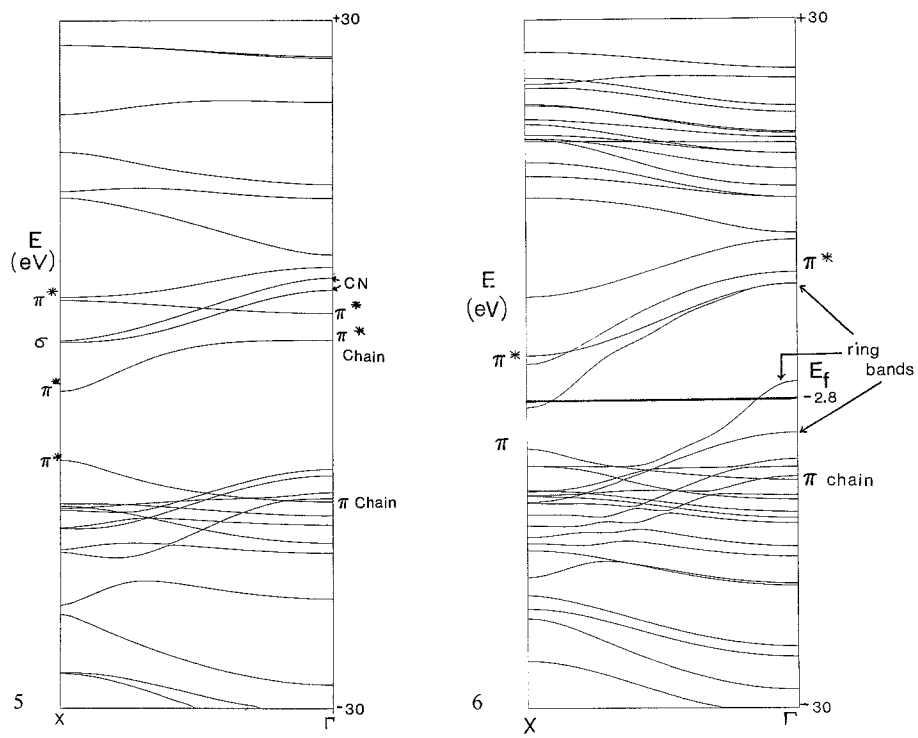

Fig. 5. Band Structure for Polycyanoacetylene, $t = 2.426$ Å
Fig. 6. Band Structure for Polyphenylacetylene, $t = 2.479$ Å, 90° ring angle

and relatively diffuse $3p$ orbitals, both carbon, and particularly nitrogen, have a contracted set. Hence, the overlap which is parallel to the main chain is unimportant and the material must rely for its electronic conductivity properties on the main chain.

2.1.4. Polymethylacetylene

Here, a model with translation distance 2.426 Å was studied. This distance does not allow the methyl groups to rotate freely and no doubt such a situation would be relieved, in practice, by C—C bond lengthening or chain twisting. For the present purpose, however, as will be seen, the effect is not important as our models are only limiting cases. The features of interest in the band structure with the former lattice vector are, (a) there is a band gap and the material is an insulator, (b) the band gap for the parent material is decreased by methyl substitution, (c) the π valence band does not necessarily lie highest in the sequence. When the lattice vector is 2.426 Å, the p_σ orbitals of the methyl carbon interact along the chain and a σ band then lies highest in the valence series. As the translation vector is increased, this σ level changes places with the normal π band (which remains unchanged and superimposable for both systems).

2.1.5. Polyphenylacetylene

For this system there are two obvious geometrical parameters to vary, firstly, the translation vector and secondly, the ring angle with respect to the main chain. Variations of both types were investigated. When the lattice parameter is set at either 2.426 Å or 2.479 Å, then the benzene rings cannot be coplanar with the main chain and must lie at an angle between 0° and 90° to it. Hence, for these translation vectors we chose the single rotation angle of 90°. Even for a translation vector equal to 3 Å the benzene rings cannot be coplanar with the backbone and, in studying the latter model, we used two twisting angles of 45° and 90°. Considering the latter cases first, the band structures show clearly that the ring bands and the chain bands are almost completely separable, as expected from symmetry: the model has insulating properties. This model affords a useful simulation of the electronic behaviour of any geometrical situation where the rings are essentially mutually non-interacting, e.g.

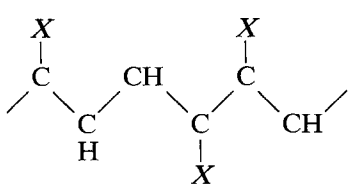

X = ring

However, twisting of the rings with respect to the chain mixes the bands and brings about considerable interaction and in the 45° model the band gap is considerably reduced. In the low-conduction region the chain π band and two ring π bands are found.

When the lattice vector is normal (i.e. 2.426 Å or 2.479 Å with the 90° twist angle), we observe a dramatic change in band structure (see Fig. 6). There is no *qualitative* difference between the two schemes based on translation vectors 2.426 Å and 2.479 Å and most of the calculated bands for the two vectors are virtually identical. However, there are splittings in the bands which stem from the phenyl rings, which seem to be significantly changed when one takes the vector to be 2.479 Å. Hence, for both the phenyl- and methoxyphenyl-substituted material, we report only the latter calculation. As in the Cl-substituted material, the π chain bands remain almost unaltered (at X they lie at -7.3 eV (valence) and 0.0 eV (conduction) with a gap of 7.3 eV). However, the face-to-face transannular interaction between the rings is very marked and this pushes the energies of the low ring-conduction bands down and the high ring-valence bands up such that they overlap and the material becomes a conductor. The Fermi level and the effective masses for the electrons and holes were calculated and are in Table 2. These valence and conduction ring bands are formed from the e_{1g} and e_{2u} orbitals of the benzene rings which are of π type in the benzene molecule. Thus, the conducting states are centred mainly on the rings and so one has an idealised picture of a conducting tube running along and parallel with the π backbone of the compound. The dramatic difference in behaviour between the benzene ring and the CH_3 and CN groups is interesting, as the latter yield insulators. The remarkable properties of the phenyl system arise from the π bands of the benzene rings which border the band gap. In neither the CN nor the CH_3 model are there such distance-sensitive bands emanating from the substituent and which occur on both sides of the band gap.

Hence, the properties of such a phenyl derivative, if it can be made, render it an interesting material for experimental study. A comparison with the known properties of a "polyphenylacetylene" is made later.

2.1.6. Poly-*p*-methoxyphenylacetylene

Because of the results obtained for the polyphenylacetylene, it is clearly of considerable interest to examine the effects of substituting groups into the benzene ring. These could enter the band structure in two ways: either by directly mutually interacting along the chain, as do the benzene rings themselves, or by modifying the π systems of the individual rings such that the "polyphenyl" conduction bands become affected. Both are of interest and, clearly, the way in which the substituent participates will be a strong function of its size, available orbitals, and the electrons it possesses. A chlorine substituent, for example, should enter the band structure in both ways whilst a substituent containing first-row atoms with saturated valencies, e.g. $-NH_2$, —Me or OMe should perturb only the ring. The latter type could, hence, be of some value as "fine-tuners" of the main conduction bands stemming from the benzene rings. In this paper we have investigated only the latter point and so, in order to find the effect of substituting the benzene ring, we calculated the structure of poly-*p*-methoxyphenyl acetylene. The band structure is shown in Fig. 7. As aforestated, the lattice

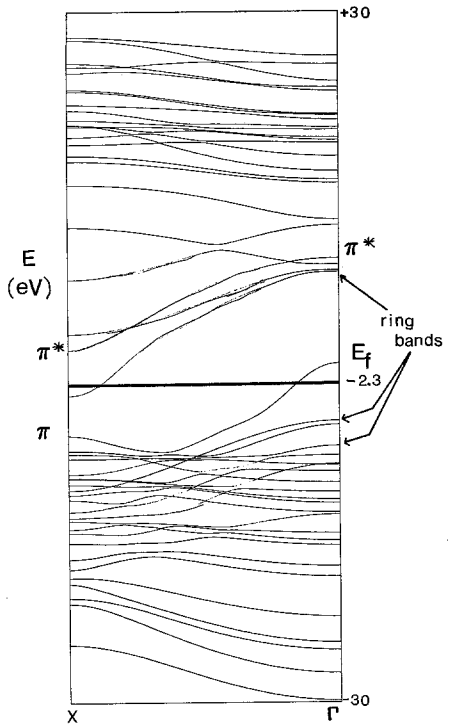

Fig. 7. Band Structure for Poly-*p*-methoxyphenylacetylene, $t=2.479$ Å, 90° ring angle

vector is 2.479 Å. The system contains eleven more bands than does polyphenylacetylene but most of the bands stemming from the MeO group are situated away from the band gap in "uninteresting" regions. The only clearly extant band which has strong oxygen character is a conduction band which lies close to the ring bands at Γ. However, this band deviates upwards towards *X*. The ring conduction band, which is partly populated, is the same width in both phenyl- and methoxyphenyl-acetylenes. This band does, however, contain a greater number of electrons in the *p* methoxypolymer (all are not absorbed in lower-lying "MeO" bands) and, correspondingly, the Fermi level is raised. Hence, the Fermi velocity of the electrons is increased by the MeO substitution, as this velocity depends directly on the derivative of E with respect to $\boldsymbol{k}$ at the Fermi level. Moreover, since the Fermi surface is also increased one expects, overall, a lower Hall constant for such a methoxy material.

2.2. Electronic Properties

The specific electronic conductivity, effective mass, and the mobility at 300 K were computed for the relevant bands of each conductor and are given in Table 2. The effective masses for both electrons and holes are given in the table for all the systems since, even for the insulators, these properties are significant for injected carriers. In all cases the effective masses of the carriers are low, which indicates that all the materials can conduct electronically if electrons (or holes) either

already exist or can be injected into the relevant bands. We observe that substitution of MeO into the phenyl ring enhances the electrical properties, mainly through increase of the density of states at the Fermi level. It is interesting that, in general, the substituents CN and methyl both induce an increase in the effective mass for both electrons and holes over the parent polyacetylene and so would be expected to reduce the conductance properties somewhat. This corresponds to a type of localisation or trapping effect by these groups. Of course, the conductivity depends also on the relevant densities of states but, if these are assumed equal in the respective π bands of the cyano-, methyl, and parent chains, then the above result holds.

For the conductors, the effective masses for electrons and holes turn out to be of the same order, although the electrons in the aromatic materials are delocalised through the rings whilst those in the chloro-compound are delocalised partly down the carbon backbone. The specific electronic conductances given in Table 2 are to be compared with that measured for graphite, i.e. $7.27 \times 10^2\ \Omega^{-1}\ \mathrm{cm}^{-1}$ [19], and the effective masses are of a similar order to those for elemental semiconductors [19].

On the former comparison, two observations must be made: firstly, the "extended-band" formula [18] makes no allowance for scattering of the electrons by any mechanism and consequent diminution of the mobility. Hence, the values for σ and μ in Table 2 must be much overestimated. We consider the effects of scattering later in this paper.

For the π main chain band of the parent compound polyacetylene and the conduction bands of the insulators, we do not know exactly at which energy point to read the density of states in order to calculate the conductivity and mobility. However, if one takes the relevant data for electrons from just above the lower edge of the conduction band and, for holes, from just below the upper edge of the valence band, one can obtain an approximate mobility (which, of course, can only be exhibited by thermal excitation or injection). For polyacetylene we obtain the values given in Table 2. Since this procedure is rather uncertain, we have not considered it worthwhile to carry it through for the other insulators.

It is clear, for the phenyl-substituted compound, that the ring "tube" is the most efficient transport medium for electrons. The conductivities exceed those of the chain by a factor of 6–10. Apart from this, the free carriers need to be first excited into the "chain" bands. However, the latter processes have a bearing on the photoconductivity of the polymers and they show that conducting states are available for electrons excited by, e.g. UV light in such materials.

It is relevant to consider the effect of the second and third dimensions of the real crystal on both our model and results. There are no full crystal structures available for these materials but some unit-cell dimensions are known and, making reasonable assumptions about the geometry of such a crystal, one can proceed further. It is reasonable to assume, as crystalline model, a simple orthorhombic system; this is consistent with published information [24] and allows the distance

apart of the chains to differ in the two other dimensions. Hence, the three-dimensional Brillouin Zone will be orthorhombic and will be of narrow cross-section because of the large inter-chain distances. The new bands along other symmetry lines of the Zone, generated by taking into consideration the other two dimensions, will necessarily be rather flat because of the limited lateral interaction between the chains over the long repeat distances. The open Fermi surface will, therefore, be elongated in the longitudinal direction. Using our results for the 1D case, it is possible to construct an approximate Fermi surface. The calculations for both phenyl and chloropolymers show bands curved in the $\Gamma - X$ direction and, clearly, the bands also will be curved in the $\Gamma - R$ and $R - M$ directions although not so markedly, since the latter directions do not coincide with the main chain axis. In all other directions, the bands will be flat. The plausible band picture in Fig. 8a allows a rough estimate of the Fermi surfaces and their areas to be made. Fig. 8b shows a sketch of the hole and electron surfaces for either the chloro- or the phenyl-substituted chain.

From these conjectures an approximate specific conductivity value can be calculated, using the formulae given by Ziman [20]. For the latter formula one needs also the melting points for the materials. We assumed the data for polystyrene and polyvinylchloride [24] to be appropriate. It was also convenient to approximate the Fermi surfaces for the two systems as a cylinder and a rectangular plate, respectively. We finally obtain the values presented in Table 3. From the density of states and the conductivity, we may obtain the mobility data.

In this calculation the mean free path, Λ, appears in the expression for the conductivity and allows for scattering to some extent. We would expect these latter conductivity and mobility data to be somewhat more realistic than the extended-band values of Table 2. It is interesting that the conductivity predicted is

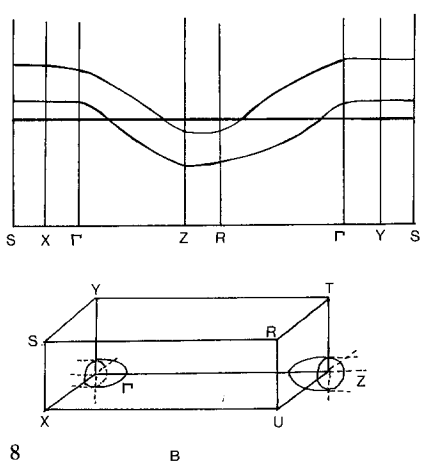

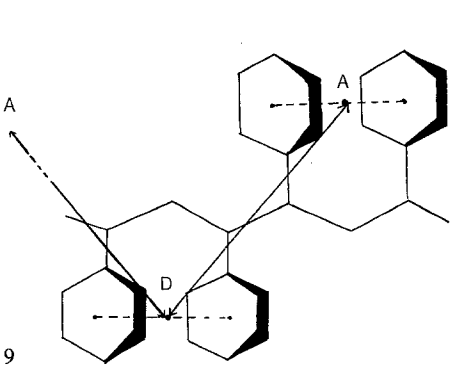

Fig. 8. Conjectural Fermi Surface for Polyphenylacetylene

Fig. 9. Model for Excitation Transfer

of the same order as the basal plane σ for graphite. (The transannular conductivity component for graphite is very small and, in this direction, the band structure resembles that of the "insulator" model of polyphenylacetylene reported here.) It is known that, for graphite, the Fermi surfaces are also small and the Brillouin Zone incorporates one narrow dimension owing to the interplate distance [21]. Hence, overall, one might expect a similarity in magnitude between the conductances of graphite and the model one-dimensional chain considered here. The one-dimensional conductivity is enhanced because the p–p overlap between the rings down the phenyl chain, being σ-type, is more effective than the π-type overlap across the graphite sheets and the density of states at the Fermi level for polyphenylacetylene is quite high also.

A better-defined estimate of the mobility may be obtained alternatively if one considers the scattering effects more closely. We cannot estimate the impurity scattering (and, indeed, it is irrelevant to our model) but, working from a polaron approach, which should be reasonably accurate for a polymer as polar as the chloro-substituted material, we may estimate the optical-mode-limited mobility. We adopt the Low and Pines approach [22] and take the optical scattering mode energies from the unit-cell fragment. For molecular chloroethylene, the important modes are the stretches involving the C—C and the C—Cl. Appropriate values for these for the present purposes are 3000 cm^{-1} and 742 cm^{-1} [23]. We also need the dielectric constants at infinite frequency in order to define the polaron effective mass. For polyvinylchloride this has value 3.29 [24]. From the Low and Pines expression we can calculate the electron mobilities relevant to each frequency for polychloroacetylene. The value given in Table 3 is the reciprocal sum of these two mobilities and is dominated by the lower frequency interaction. This mobility is, of course, much lower than the extended band value but comparable with that obtained using the mean free path from the "Lindemann melting formula" [20].

From both conductivity and mobility one can obtain the Hall constant for each type of transport, since $R = \sigma\mu$. The sign of this latter quantity, as calculated, corresponds to the type of carrier (positive for electrons, negative for holes). For brevity, and because the possible errors in the calculation of μ and σ make it unwarranted, we do not report the actual figures here. However, qualitatively in the chloro-conductor the Hall constants for electrons and holes contribute separately and, overall, one finds an aggregate value which shows that electrons and holes are fairly evenly balanced as carriers in the materials.

Early experimental work [31] on the electronic conductivity of amorphous polyphenyl- and poly-*p*-methoxyphenylacetylene afforded low values for the electrical conductivity of these materials. This was interpreted as stemming from the ease of backbone segmental rotation which breaks the conjugation and introduces the need for electron hopping from section to section of the chain. The energy of activation was measured as ~20 kcal $mole^{-1}$. In the polymers studied, the highest molecular weight recorded was 5000 for poly-*p*-methoxyacetylene, which corresponds to ~38 monomer units in a chain of maximum length of

~100 Å. Hence, even if these chains were oriented directly in line lengthwise between the electrodes and the film thickness were 0.1 mm, then there would be $\sim 10^4$ molecules and a corresponding number of breaks between the chains. This barrier to transfer of an electron would add considerably to that stemming from lack of bond conjugation. However, North and Hankin's work illustrates how the electrical conductivity can be limited in a real case. It is clearly of great importance experimentally to prepare films as fully regular and orientated as possible, in which the polymers have a very high molecular weight. It is interesting that, in experiments where the "polyphenylacetylene" used contained a fraction with high molecular weight, singlet energy transfer down the chain was effectively instantaneous [5]. This is discussed further later.

2.3. General Conclusions

Our choice of substituents enables us to be able to extract a few general principles which can perhaps be applied in experimental design of future materials. Firstly, alkyl groups attached to the chain act in an "inert" manner and, if anything, detract from the electronic properties. Indeed, we also find the same effect from the cyano-group and, hence, we expect small side groups built from first-row atoms to be, in general, ineffective in enhancing the electronic properties. Atoms from the second and subsequent Periodic rows, directly attached to the chain, should have interesting properties, particularly if they are electron donors. Such atoms distort the bands around the gap by their bonding parallel to the chain; they also provide electrons for the conduction bands.

All aromatic systems should yield the same type of transannular overlap and conductance bands calculated in this paper. Since benzene is the smallest such ring, no other geometry for the polymer is expected. We are not able to analyse fully the effect of substituents in the ring at the present time – many more calculations would be needed. However, taking MeO as a typical example of a π donor and σ acceptor, we expect such groups to increase the Fermi velocity of the highest electrons, concomitantly decreasing the Hall constant and enhancing the conductance. This effect should be effectively independent of position of substitution in the phenyl ring. The NR_2 group would clearly be of some interest in this context. Electron-π-accepting substituents (e.g. $-BR_2$) should leave the Fermi level unaltered but will produce a lowering of the conduction band levels and reduce the gap. Indeed, the diffuse π orbital of boron may well, like Cl, be directly instrumental in the conduction process (unlike the MeO-group bands which are displaced above the ring bands).

2.4. Comparison with Polystyrene

It is well known that polystyrene is a non-conductor of electrons and this can readily be attributed to the large band-gap which arises in such saturated polymers (cf. polyethylene, polyvinylchloride [8]). Moreover, the phenyl rings can be staggered with respect to each other down the chain and, finally, sections of the chain can perform facile segmental rotation. Although the polyene chain can

certainly adopt both *trans* and *cis* geometries, the "stiffness" of the chain (coming from the π bonding) tends to oppose segmental rotation in the solid. In polystyrene, an excitation induced in one ring can be transferred along the chain from site to site by a Förster mechanism involving excitons [25]. Although excitons have been considered [5, 6] as a possible mode of energy-delocalisation mechanism in the polyphenylacetylenes, it was found that energy transfer along the chain is essentially instantaneous and that the transfer distance is as long as a segment of continuous conjugated polymer chain. This corresponds essentially to the present result. The same type of terms which produce the extended band states of the present model also govern energy transfer. Hence, one would expect from our model to find rapid energy transfer down the polymer chain.

2.5. Effects of Perturbation

2.5.1. Rotation of the Polyene Chain

In the solid state polyacetylene is known to be the most stable in the all-*trans* configuration [26], although the *cis* form can be made. The geometry of the *cis* form does not affect the continuity of conjugation down the polymer chain but the possible positioning of substituents becomes strongly affected. Thus, ideal head-to-tail polymerisation of CH≡CR in a *cis* manner would produce a polymer with *R* groups on opposite sides of the main chains (indeed, it would hardly be geometrically feasible to produce a phenyl-substituted *cis* polymer with rings on the same side). This means that the rings in a *cis* head-tail polymer will be mutually electronically isolated and the broad electronic bands stemming from the rings described earlier in the all-*trans* model will not exist. Ideal head-tail polymerisation into an all-*trans* chain yields the model polymer with which this work is concerned. The polymers studied experimentally in fluid and in the amorphous state [5, 6] are unlikely to have the all-*trans* configuration, although they are all probably mostly of head-to-tail type. Again, it must be emphasised that orientation of the crystal is clearly a prime factor affecting electrical properties.

We note that any segmental *trans*-to-*cis* rotation of the chain in the all-*trans* model will also break the continuity of the transannular phenyl group system, although such rotation (even if it is not complete) affects little the conjugation along the backbone chain. In the solid state, such segmental rotation is restricted (though said to be facile in solution [5, 6]) and will require quite high activation energy. Even the opposite, more favoured, *cis-trans* transformation in polyacetylene is reported to require 17–40 kcal mol^{-1} [26]. A limited number of *trans-cis* rotations in the chain, such as will be found around room temperature, will not be important and will produce only a minute set of isolated impurity levels formed from the displaced groups. Electron movement between sequences at these points would become hops. In a polymer where *all* rings were isolated (as in the *cis* head-tail compound) the electronic properties should revert essentially to those of the parent chain. Hence, the onset of light absorption and photoconductivity would depend mostly on the backbone, since these states would now lie in

the same energy region as the benzene states. The quasi-benzene *orbital levels*, stemming from the isolated rings, would then be spread over narrow ranges in the valence and conduction bands.

The effect of random head-tail or head-head polymerisation on the properties of the material is, clearly, very important. Such a material will possess sequences in which the phenyl rings are aligned for delocalisation, the number of rings varying, as well as regions where they will be electronically isolated from each other. The backbone conjugation will, however, still exist. It is a general feature of conjugated systems that the energy of light absorbed decreases as the sequence of coupled chromophores lengthens. Hence, the longer sequences of aligned phenyl rings should show longer wavelength absorption, producing a range of excimer states. So, the overall energy-level picture of such a random polymer is of, first, a background, essentially unaltered, series of bands emanating from the backbone chain. Superimposed on these bands are (a) "insulator" benzene levels (isolated rings) lying in very narrow ranges around the band gap and (b) the lower-lying excimer levels stemming from ring sequences. These latter will form a broader band of impurity levels (some quite localised) within the original band-gap. Since such a polymer lacks the "ring conduction bands" of the idealised structure, then absorption and emission of light over a rather broad range of wavelengths could be brought about by the presence of these excimer levels instead. The excitations could then be delocalised by Förster transfer to other sequences or to isolated rings, and by transference of the excitation to the main chain: the latter process could then excite electrons into the extended conduction states associated with the backbone and would involve mainly the higher energy excitations. Moreover, since the main chain is always at least partly conjugated, it sets up no basic barrier to the photoconductivity stemming from electron delocalisation.

Migration of electrons excited in the latter way into the polymer chain states is an efficient process and can compete effectively with the retarding and quenching effects, e.g. relaxation to the lattice and light emission.

2.5.2. Energy Transfer in the Perturbed Polymer

The transfer of singlet energy from ring sequence to ring sequence (the sequences having from 1 to n rings) under the control of Förster kinetics will clearly be more subject to the above retarding effects. Moreover, energy transfer of this type requires, for its effectiveness, definite matching spectral characteristics in the excited donor and acceptor. These spectral properties depend on the sequence length and so, in a random set of sequences, ideal transfer conditions may seldom be found. This restriction will, however, be somewhat relaxed for the important long sequences, since for these the absorption and emission spectra are broader. Moreover, since the resonance interaction between states on *juxtaposed* rings is large, then the coupling is, in the Förster sense, "strong" and the transfer rate from sequence to sequence enhanced. The transfer process in such a case is thus a type of exciton transfer, although the random nature of the donating and accepting groups makes such an exciton somewhat difficult to define. (Along the

backbone, of course, the term is irrelevant, as here we have extended band states.) In both the low-energy and the high-energy light-stimulated regions, we expect rapid energy delocalisation, in the former through the ring sequences and in the latter down the main chain.

Because of their electronically localised nature the "single", isolated, phenyl side groups will act, relatively, as trapping sites for the excitation; the latter will then be quenched by non-radiative relaxation.

We can proceed further and obtain a quantitative description of such a process. It is of some interest to calculate the efficiency of transfer of an excitation from one group to another in such a polymer under the control of Förster kinetics. In order to do this, we need to know the relevant absorption and emission energies of side group sequences to be considered. The simplest model which will yield useful information is the set of "dimer" groups shown in Fig. 9. These are designated "A" and "D" (standing for acceptor and donor). The pairs of phenyl rings form excimer states by transannular interaction and the transfer efficiency will be strongly dependent on both the energies of these states and the associated oscillator strengths for absorption and emission involving them. We calculated the electronic structure for the important states generated by the ring π systems by means of the standard Pariser–Parr–Pople technique [27, 28], using input parameters given previously [29]. The value for the interring $p_\pi p_\pi$ interactions was -0.6 eV [30]. The model used was a fragment of the main chain and contains two rings. Configuration interaction between eight bonding and eight antibonding orbitals was included in the calculation of the excited states and oscillator strengths. For brevity, the results are not detailed here but the two lowest singlet states of importance have energies, oscillator strengths and lifetimes, 4.05 eV, $f = 1.4 \times 10^{-4}$; $\tau = 1.0 \times 10^{-5}$ sec and 4.70, $f = 1.22 \times 10^{-2}$, and 1.1×10^{-9} sec (we call these states: A, D and A', D'). These values may be used in conjunction with the elegant general theory of excitation transfer [25] developed by Förster. The distances between the excimer centres in the model (Fig. 9) (7.39 Å) make it appropriate to treat the situation under the "weak transfer" scheme [25], which involves vibronic coupling in the excited states.

We suppose that the excimer state lying at 4.7 eV (i.e. similar to the parent benzene $^1B_{2u}$ state) is excited together with a progression of vibrational quanta. This energy is then transferred to the other vibrational state of the electronic states of the next pair of phenyl rings lying some 7 Å away. The two receptor sites in Fig. 12 (which contribute additively) both have geometrical orientation factor, K^2, [25] = 1.61. The transfer efficiency in Förster theory is governed by the overlap between the absorption spectrum of the acceptor molecular site (A) and the fluorescence spectrum of the donor site (D) and one can define a "critical transfer distance", R_0, over which the excitation can be spread. R_0 corresponds to a situation where a single transfer between molecules can be made in the fluorescence lifetime of D. The quantity R_0 is vital in order to assess the efficiency of delocalisation of the excitation down the molecular chain. For the two calculated states, the fluorescence lifetimes can be calculated directly from the

Einstein coefficients for spontaneous emission. The values obtained are 10^{-5} sec and 1.1×10^{-9} sec for the 4.05 and 4.70 eV states, respectively. Since the excitation transfer must compete with deactivation *via* excimer emission, transfer from a state to another site must be effective within the fluorescence lifetime. From the calculated spectroscopic data, we can compute the resonance interaction term between the excited-state pairs $D'-A$ and $D'-A'$ for the inter-excimer distance. This represents the picking up of energy by the state (D') (which is almost an isolated benzene state, being the out-of-phase linear combination of two ring states) and its transfer to a similar state or to a bonding excimer state. Under the "weak coupling" scheme [25], one must take account of the overlap between the vibrational wave functions of the donor and acceptor. Our model assumes transfer from a progression of vibronic states of D to the equivalent states of A. The first experimental electronic band of benzene ($^1B_{2u}$) carries with it a long progression ($\sim$5 quanta) of the totally symmetric A_{1g} vibration combined with a single E_{2g} vibration which serves to allow the electronic transition. Hence, in implementing the calculation we must consider these vibronic states.

We select a number of vibrational quanta as 5 for both D and A, since this corresponds roughly to the structure of the first benzene band. We calculated the 36 vibrational overlap terms and, from them and the data for the electronic states (*vide supra*) obtained values for the transfer $D'-A$ as: $k_{D'A'}(\text{sec}^{-1})=2.0\times10^{12}$; $R_0=27$ Å and for the transfer $D'-A'$ as $k_{D'A'}(\text{sec}^{-1})=1.8\times10^{13}$; $R_0=38$ Å. The R_0 values are to be compared with the critical transfer distances measured by North, Ross, and Treadaway for solid polyphenylacetylene [6] from fluorescence experiments. For the transfer from $D'-A'$ we find an R_0 value in satisfyingly good agreement with that afforded by the experiment (44 Å). The results show, also, that the transfer distance between the dimer units is well attainable within the excited-state lifetime and can compete effectively with fluorescence deactivation. In addition, we computed the R_0 values for other energy transfers. The results are not given in detail here but it is notable that all possible transfers can be accomplished within the excited-state lifetimes. Indeed, for transfer between the low-lying excimer states (D and A) the transfer distance equals $\sim10\times D-A$ distances, even though the oscillator strength of this state is small. This stems from the rather longer lifetime of this excited state. The model dimer considered here is the smallest excimer unit possible and, as aforesaid, there will be longer ring sequences in the real material. Hence, absorption will occur at lower energy. Since the relaxation time, τ, is inversely proportional to the square of the energy, then longer lifetimes and longer migration distances occur in the real system. Thus, in the prepared polymer, we would expect a wavelength dependence of the transfer distance, the latter increasing with the wavelength of light emission.

2.6. The Density-of-States and Joint-Density-of-Sates Curves

These two functions were calculated for all the systems investigated. For brevity, the plots are not reproduced here and we give as typical examples, the DOS and JDOS curves for the phenyl conductor (Figs. 10 and 11). For the insulators we expect the lowest-energy electronic transitions to be those of the polyene chain or,

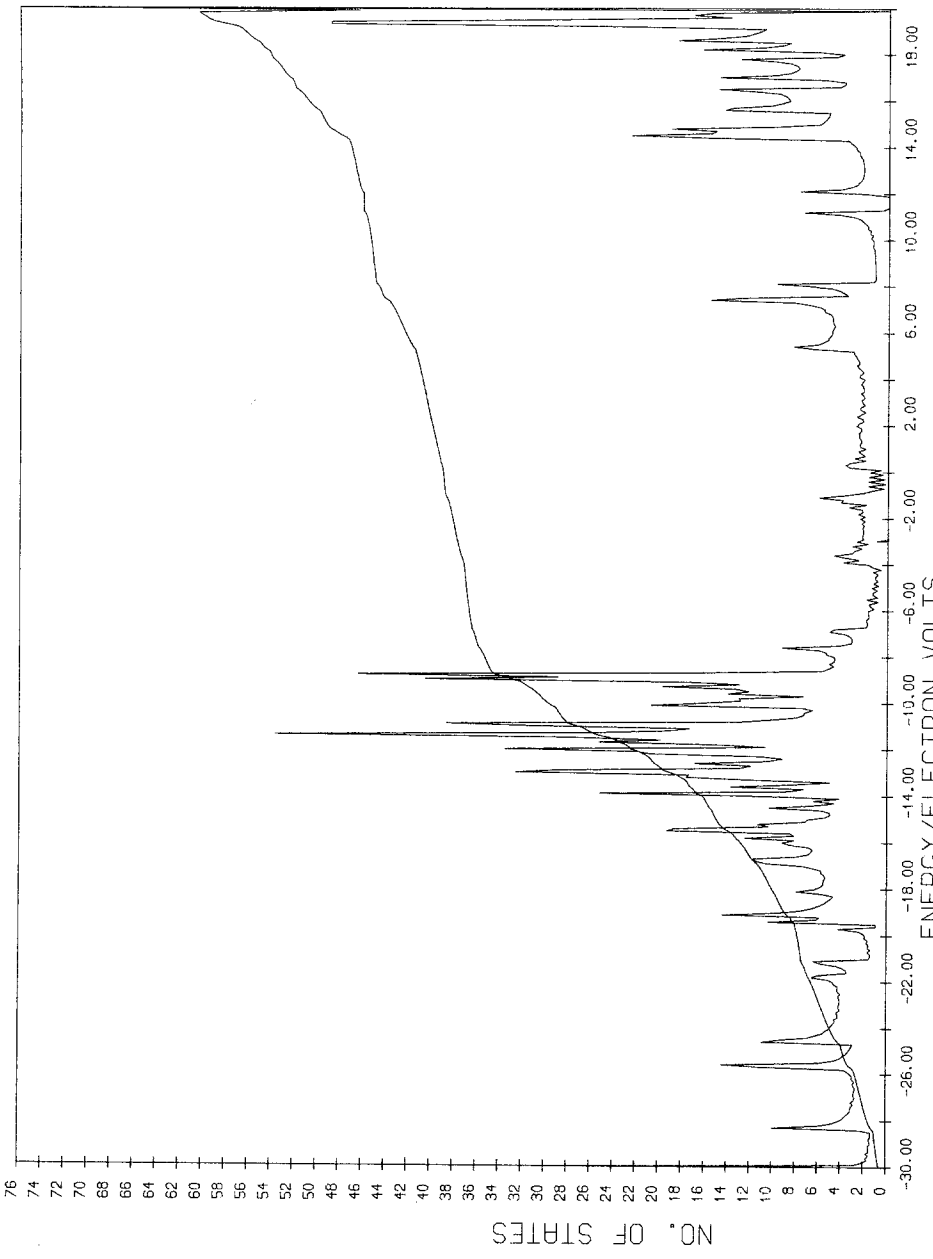

Fig. 10. Total Density of States for Polyphenylacetylene (Conductor)

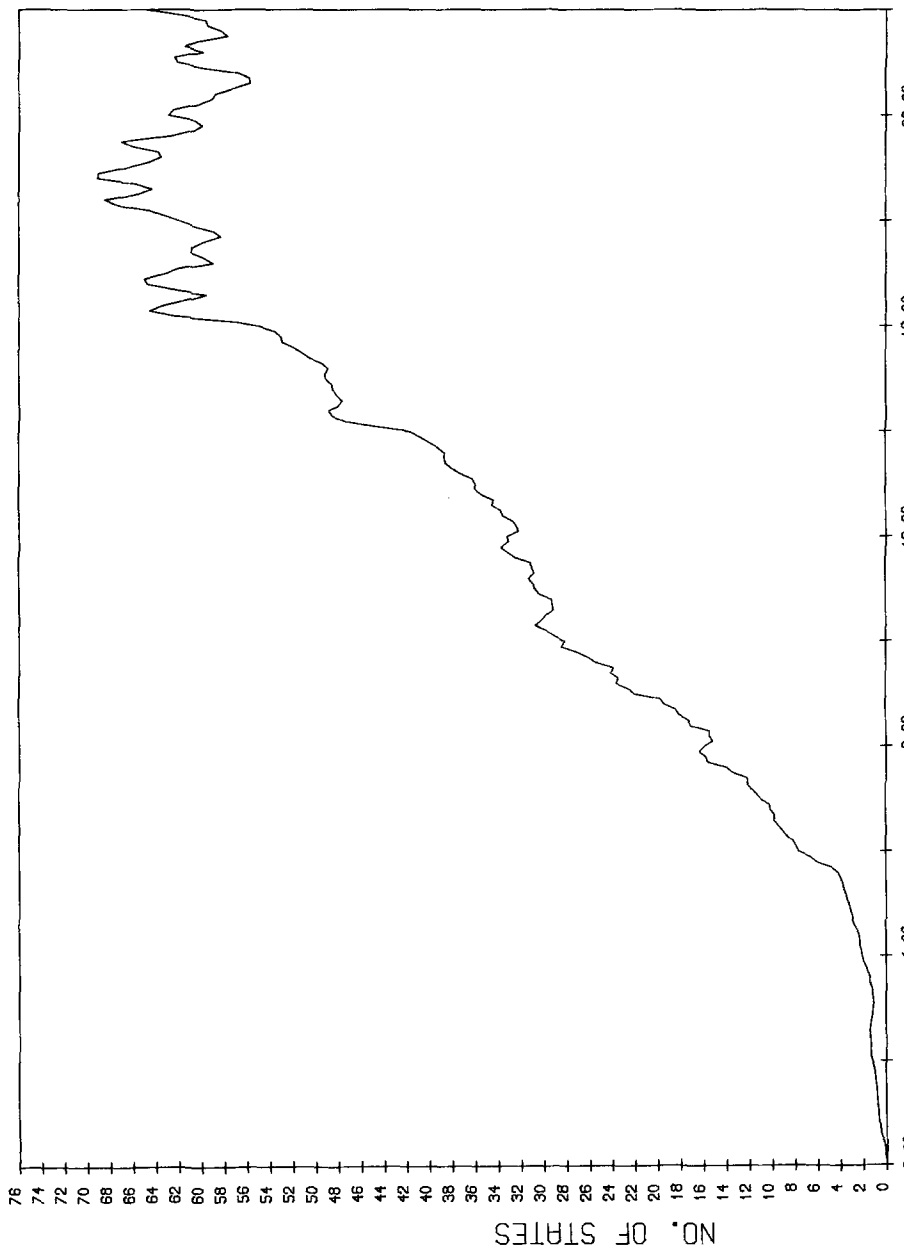

Fig. 11. Joint Density of States for Polyphenylacetylene (Conductor)

as in the case of the phenyl-substituted compound, the exciton states of the attached side groups. It is clear that the band-gap of System 4*b* is considerably larger than the known experimental energy for the first benzene transition band. This is not surprising because the band-gap represents merely an eigenvalue difference for a set of *quasi*-accidentally degenerate benzene π orbitals. What, of course, the present calculation does not include is the electronic interaction between the excited states and, for the case in point, this is quite important. With the inclusion of electronic interaction the energies of states generated from these ring eigenvalues will reduce to the 4–5 eV region as required to correlate with the spectrum of a monosubstituted benzene molecule.

When one considers the conductors, the electronic-interaction problem vanishes as the states are now fully extended band states. If we neglect the $\boldsymbol{k}$-conservation selection rule for the moment, then the absorption starts at zero eV and increases, at first slowly, but very rapidly at higher energy. Our joint-density-of-states calculation does not include the matrix elements of the dipole moment operator and so we are unable to correctly scale the low-energy spectral profiles. However, we know from the general nature of the Bloch functions that, e.g. for the chlorine-substituted chain, the low-energy part of the spectrum (up to 5 eV) is likely to be more intense than the succeeding 4 eV as the former involves charge-transfer transitions from chlorine to the chain. When the $\boldsymbol{k}$-selection rule is enforced, a rather subtle effect operates on the spectra of these conductors. Although the valence and conduction bands overlap, the $\boldsymbol{k}$-selection rule forbids any transition between filled states at the top of the valence band and empty ones in the conduction band. Moreover, no low-energy transitions can occur *within* the high-valence band and or part-filled conduction band as these would also violate the rule. Hence, e.g. for the phenyl-substituted chain, the lowest $\boldsymbol{k}$-allowed energy transition occurs at the Γ point and is of energy 3.8 eV. Of course, in practice some absorption will occur at wavelengths below this due to the chain-twisting effects discussed earlier. Experimentally [6], "polyphenylacetylene" starts to absorb near 400 nm (3.0 eV) and the absorption rises, exhibiting shoulders though no definable peak, as far as 6.2 eV. This corresponds generally to the behaviour expected from our calculation, although detailed interpretation is obviously unprofitable. We do know, however, that for the phenyl-substituted compound the lowest-energy transitions lie essentially within the conjugated phenyl ring band system and they arise, as in the benzene molecule, from $\pi - \pi^\star$ states. This low-energy spectral region therefore contains the strong band deriving from the $^1E_{1u}$ state of the isolated molecule. Thus, we would expect absorption to be strong in the region from 3.5–6 eV.

It is known [5, 6] that polyphenylacetylene absorbs light over a wide range of energy and will remit this as longer-wavelength fluorescence. In solution the emission band is narrow and lies at longer wavelength than the absorption but, in the solid state, the band is considerably broader and extends into the absorption region. This observation is in line with our results. We expect emission to be possible from the excimer states as a process which competes with further down-chain energy transfer. The broadness of the band will reflect the distribution of these states.

2.7. *Effects of Doping with Foreign Atoms*

It is known [32] that doping of polyacetylene with compounds such as iodine and AsF_3 causes its electronic conductivity to rise by several orders of magnitude. A case in point is the result shown by intercalated iodine atoms. It is believed [32] that these atoms are intercalated into half the chain sites as I_3^- or I_5^- chains by displacement of the polyacetylene chains. We can comment on these materials from our calculations on the band structures of polychloroacetylene and polyacetylene. From the former, we know that halogen atoms placed along the chain (in our case directly attached) mutually interact and form wide bands. They also distort the conduction band of the main chain. Even undistorted, this latter conduction band of polyacetylene is available as a convenient path for electrons from the substituents or dopants to be delocalised. Hence, one could regard the donor dopant atoms as merely a source of electrons which can be injected into the polyacetylene conduction bands. Alternatively, electron acceptors can take electrons in from the polyacetylene valence bands, thus inducing hole conduction. The key point is that the conduction media, populated, respectively, by electrons or holes, are the broad, efficiently conducting bands of the polyacetylene chain. At present, the absolute energy positions of such donor and acceptor states are not known: however, the electron affinity of a single I^- ion is about 3.2 eV [33]. This means that the interaction bands from associated iodines will lie near to our calculated conduction band. On the other hand, the lowest *empty* levels of the acceptor AsF_3 will lie near ~ -8 eV and so will be conveniently situated energetically for accepting electrons from the valence band of the chains. Hence, our results afford a natural explanation for the observations.

Acknowledgments. One of us (E.A.C-V.) thanks the Royal Society and the Academia de la Investigación Científica, A.C. (México) for the award of a Grant. The work was performed during Leave of Absence (of E.A.C-V.) from the Instituto de Investigaciones en Materiales, U.N.A.M., México D.F. We would like to thank Prof. A. M. North for valuable comments.

References

1. Shirakawa, H., Louis, E. J., MacDiarmid, A. G., Chiang, C. K., Heeger, A. J.: Chem. Commun. 578 (1977)
2. Chiang, C. K., Fincher Jr., C. R., Park, Y. W., Heeger, A. J., Shirakawa, H., Louis, E. J., Gau, S. C., MacDiarmid, A. G.: Phys. Rev. Lett. **39**, 1098 (1977)
3. Chiang, C. K., Druy, M. A., Gau, S. C., Heeger, A. J., Louis, E. J., MacDiarmid, A. G., Park, Y. W., Shirakawa, H.: J. Amer. Chem. Soc. **100**, 1013 (1978)
4. Clarke, T. C., Geiss, R. H., Kwak, J. F., Street, G. B.: Chem. Commun. 489 (1978)
5. North, A. M., Ross, D. A.: J. Polym. Sci. Symposium No. **55**, 259 (1976)
6. North, A. M., Ross, D. A., Treadaway, M. F.: Europ. Polym. Journal **10**, 411 (1974)
7. A partial list of relevant references are to be found in Karpfen, A., Petkov, J.: Theoret. Chim. Acta (Berl.) (1979)
8. McAloon, B. J., Perkins, P. G.: J. Chem. Soc. (London), Faraday Trans. **II**, 68, 1121 (1972)
9. Hoffman, R.: J. Chem. Phys. **39**, 1397 (1963)
10. Pople, J. A., Segal, G. A., Santry, D. P.: J. Chem. Phys. **43**, S129 (1965)
11. Karpfen, A., Petkov, J.: Solid State Comm. **29**, 251 (1979)

12. Marwaha, A. K., Perkins, P. G., Stewart, J. J. P.: Theoret. Chim. Acta (Berl.) **57**, 1 (1980)
13. Perkins, P. G., Stewart, J. J. P.: J. Chem. Soc. (London), Faraday Trans. **II**, **76**, 520 (1980)
14. Interatomic Distances in Molecules and Ions, Chem. Soc. Special Publ. Chem. Soc. (London) (1958)
15. Burns, G.: J. Chem. Phys. **41**, 1521 (1964)
16. Armstrong, D. R., Jamieson, J., Perkins, P. G.: Theoret. Chim. Acta (Berl.) **49**, 55 (1978), Theoret. Chim. Acta (Berl.) **50**, 1134 (1978)
17. Levison, K. A., Perkins, P. G.: Theoret. Chim. Acta (Berl.) **14**, 206 (1969)
18. Mott, N. F., Davis, E. A.: Electronic processes in non-crystalline materials, Oxford University Press (1971)
19. Handbook of Chemistry and Physics, 56th Edition, Ed. R. C. Weast, Chem. Rubber Publishing Coy., Cleveland, Ohio, U.S.A.
20. Ziman, J. M.: Electrons and phonons, Oxford University Press (1960)
21. Slater, J. C.: Symmetry and energy bands in crystals, New York: Dover Publications 1972
22. Low, F. E., Pines, D.: Phys. Rev. **98**, 414 (1955)
23. Lambert, J. B., Shurvell, H. F., Verbit, L., Cooks, R. G., Stout, G. H.: Organic structural analysis, New York: Macmillan 1976
24. Polymer Handbook, 2nd Edition, Eds. J. Brandrup, E. H. Immergut. New York: Wiley (1975)
25. Förster Th. in Modern quantum chemistry Part III, Ed. O. Sinanoglŭ. New York: Academic Press (1965)
26. Ito, T., Shirakawa, H., Ikeda, S.: J. Polym. Sci. **13**, 1943 (1975)
27. Pariser, R., Parr, R. G.: J. Chem. Phys. **21**, 466 (1953)
28. Pople, J. A.: Trans. Faraday Soc. **49**, 1375 (1953)
29. Armstrong, D. R., Perkins, P. G.: Theoret. Chim. Acta (Berl.) **5**, 215 (1966)
30. Value calculated from $P_\sigma P_\sigma$ overlap at the appropriate interatomic distance
31. North, A. M., Hankin, A. G.: Trans. Faraday Soc. **63**, 1525 (1967)
32. Baughman, R. H., Hsu, S. L., Pez, G. P., Signorelli, A. J.: J. Chem. Phys. **68**, 5406 (1978)
33. Ionic crystals, lattice defects and nonstoichiometry, London: N. N. Greenwood, Butterworth (1968)

Received April 21, 1980/October 22, 1980